Polymer structure and property effects on solid dispersions with haloperidol: poly(N-vinyl pyrrolidone) and poly(2-oxazolines) studies

Polymer structure and property effects on solid dispersions with haloperidol: poly(N-vinyl pyrrolidone) and poly(2-oxazolines) studies

Xiaoning Shan, Adrian C. Williams, Vitaliy V. Khutoryanskiy*

Reading School of Pharmacy, University of Reading, Whiteknights, PO Box 224, Reading RG66AD, United Kingdom, email: v.khutoryanskiy@reading.ac.uk

Abstract:

Poly(2-methyl-2-oxazoline) (PMOZ), poly(2-propyl-2-oxazoline) (PnPOZ) and poly(2-isopropyl-2-oxazoline) (PiPOZ) were synthesized by hydrolysis of 50 kDa poly(2-ethyl-2-oxazoline) (PEOZ) and subsequent reaction of the resulting poly(ethylene imine) with acetic, butyric and isobutyric anhydrides, respectively. These polymers were characterized by proton nuclear magnetic resonance, FTIR spectroscopy, powder X-ray diffraction, and differential scanning calorimetry. The poly(2-oxazolines) as well as poly(N-vinyl pyrrolidone) (PVP) were used to prepare solid dispersions with haloperidol, a model poorly soluble drug. Dispersions were investigated by powder X-ray diffractometry, differential scanning calorimetry and FTIR spectroscopy. Increasing the number of hydrophobic

groups (-CH_2- and -CH_3) in the polymer resulted in greater inhibition of crystallinity of haloperidol in the order: PVP > PnPOZ=PEOZ > PMOZ. Interestingly, drug crystallization inhibition by PiPOZ was lower than with its isomeric PnPOZ because of the semi-crystalline nature of the former polymer. Crystallization inhibition was consistent with drug dissolution studies using these solid dispersions, with exception of PnPOZ, which exhibited lower critical solution temperature that affected the release of haloperidol.

Keywords: solid dispersions, poly(N-vinyl pyrrolidone), poly(2-oxazolines), crystallinity, hydrophobic drug, amorphous, haloperidol.

1. Introduction

Approximately 40 % of approved drugs and almost 90 % of newly developed active ingredients are poorly soluble in water (Kalepu and Nekkanti, 2015). Therefore, the development of new medicines using these hydrophobic drug molecules present a challenge for formulation scientists.

Several approaches are currently being exploited to improve the solubility and dissolution profiles of hydrophobic drugs. These include the use of inclusion complexes with cyclodextrins (Carrier et al., 2007; Conceicao et al., 2018; Morrison et al., 2013), formation of salts (He et al., 2017), co-

crystals (Blagden et al., 2007), hydrotropic agents (Kim et al., 2010), micellar structures (Qu et al., 2006; Volkova et al., 2019) as well as solid dispersions (Brough and Williams, 2013; Singh and Van den Mooter, 2016).

Solid dispersions are defined as physical mixtures of poorly-soluble drugs with some hydrophilic materials (Vasconcelos et al., 2016) and include eutectic systems, solid solutions (which themselves can be continuous or discontinuous depending on component miscibility) and systems where a drug can be in an amorphous or partially crystalline state in an amorphous or crystalline carrier. Several classes of hydrophilic polymers have been exploited to prepare amorphous solid dispersions, including poly(N-vinyl pyrrolidone) (Knopp et al., 2016; Li and Buckton, 2015; Niemczyk et al., 2012), cellulose ethers (Chavan et al., 2019), polyethylene oxide (Abu-Diak et al., 2012; Ozeki et al., 1997) and poloxamers (Ali et al., 2010). In some studies, the reduction of drug crystallinity in solid dispersions with various polymers has been explored and related to the chemical structure and properties of water-soluble polymers. For example, in a series of studies of solid dispersions prepared from ibuprofen and PVP, it was demonstrated that reduced drug crystallinity was due to hydrogen bond formation between drug molecules and the polymer (Niemczyk et al., 2012; Rawlinson et al., 2007; Williams et al., 2005). However, systematic studies into the effects of polymer structures on their ability to reduce drug crystallinity are currently lacking because there are limited opportunities

to vary polymer structures in a controlled manner; most studies use commercially available polymers.

Haloperidol is an antipsychotic drug used to treat schizophrenia, delirium, nausea and vomiting, and other neuropsychiatric disorders (Chaparro et al., 2013; Krause et al., 2018; Zayed et al., 2019). It is a poorly-soluble drug that is commonly formulated as solutions for oral administration or injections, and also as tablets (Demoen., 1961). Previously, solid dispersions with haloperidol were prepared using different weak organic acids (Lee et al., 2017; Singh et al., 2013), PVP (Saluja et al., 2016) and polyethylene glycol (Baird and Taylor, 2011) and dispersions have been made into free flowing tabletable powders by combining with mesoporous metalosilicate (Shah and Serajuddin, 2015).

Poly(2-oxazolines) are an emerging class of polymers, currently attracting substantial interest due to a number of unique physicochemical properties and lack of toxicity (de la Rosa, 2014; Hoogenboom, 2009; Lorson et al., 2018). Lower members of the poly(2-oxazoline) family exhibit solubility in water: poly(2-methyl-2-oxazoline) (PMOZ), poly(2-ethyl-2-oxazoline) (PEOZ), poly(n-propyl-2-oxazoline) (PnPOZ) and poly(isopropyl-2-oxazoline) (PiPOZ). Recently, poly(2-oxazolines) were used to prepare solid dosage forms as individual polymers and also in combination with some other pharmaceutical excipients (Boel et al., 2019; Fael et al., 2018; Moustafine et al., 2019; Ruiz-Rubio et al., 2018).

Using different water-soluble poly(2-oxazolines) to design solid dispersions offers interesting and previously unexplored opportunities to understand the effect of polymer molecular structure and hydrophilic-hydrophobic balance on the crystallinity of a dispersed drug. In this study, a series of water-soluble poly(2-oxazolines) were synthesized with equivalent degrees of polymerization by hydrolysis of commercially-available PEOZ into linear poly(ethylene imine) (PEI) and subsequent conversion into PMOZ, PnPOZ and PiPOZ. The structure and properties of the resulting polymers were studied by spectroscopic (^{1}H NMR and FTIR spectroscopies), thermal (differential scanning calorimetry) and powder X-ray diffraction methods. These materials were then used to prepare solid dispersions of haloperidol, a model poorly-soluble active pharmaceutical ingredient, and the effects of polymer structure on drug crystallinity and drug dissolution profiles were explored and compared to PVP-based solid dispersions as a control.

2. Materials and methods

2.1. Materials

Poly(2-ethyl-2-oxazoline) (PEOZ) 50 kDa (polydispersity index, PDI 3-4), poly(N-vinyl pyrrolidone) (PVP) 55 kDa (K-value 30), butyric anhydride

(≥97.0 %), isobutyric anhydride (≥97.0 %), haloperidol (HP) were from Sigma-Aldrich (UK). Hydrochloric acid (37 wt %), N,N-dimethylacetamide (DMA), acetic anhydride (≥99.0 %), triethylamine (TEA, 99.7%, extra pure), sodium hydroxide were from Fisher Scientific (UK). Dialysis membrane with a molecular cut-off 3.5 kDa was from Medicell International Ltd., UK.

2.2. Synthesis of PEI

PEOZ was hydrolyzed to linear PEI according to a procedure reported by (Sedlacek et al., 2019a). Specifically, PEOZ (20.0 g) was dissolved in 200 mL 18 wt % aqueous hydrochloric acid and heated overnight for 14 h at 100 °C. The PEI solution obtained in hydrochloric acid was then diluted with ice-cold distilled water (1 L). Ice-cold aqueous sodium hydroxide (4M) was added dropwise to the solution of PEI. Initially PEI solution remained soluble, but with further addition of NaOH the PEI precipitated at pH 10-11. The precipitate was filtered off and washed twice with distilled water and re-precipitated twice then dried under vacuum to obtain PEI as a white power (yielding 7.6 g (87%)). This material was analyzed by ^{1}H-NMR, PXRD, DSC and FTIR.

2.3. Synthesis of PMOZ, PnPOZ and PiPOZ

PMOZ, PnPOZ and PiPOZ were synthesized according to a procedure developed by (Sedlacek et al., 2019b) for the synthesis of high molecular

weight PMOZ. PEI (1 eq. of amines, 1.0g) was dissolved in DMA (20 mL) upon heating. The mixture was cooled in an ice-water bath (a fine suspension of PEI appeared) and acetic anhydride (2.5 eq, 5.4 mL), butyric anhydride (2.5 eq, 9.4 mL) or isobutyric anhydride (2.5 eq, 9.6 mL) was then added, resulting in immediate dissolution of PEI. TEA (2.5 eq, 4.8 mL) was added. The reaction mixture was purged with nitrogen and allowed to stir at 0 °C for 1 h and then at room temperature overnight. The obtained mixture was then diluted in deionized water and purified by dialysis (MWCO 3.5 kDa) at room temperature for PMOZ and PiPOZ and in a fridge (～5°C) for PnPOZ. All polymers were recovered by freeze-drying as white solids (yields 89.4%, 88.5% and 88.9% for PMOZ, PnPOZ and PiPOZ, respectively).

2.4. Calculation of hydrophilic-hydrophobic balance (HHB) values for polymers

HHB values for all polymers were calculated according to the following equation taken from (Khutoryanskiy et al., 2004):

$$HHB = \frac{\sum N_i * EN(carbon,hydrogen)_i}{\sum N_i * EN(oxygen,nitrogen)_i} \qquad (1)$$

where N_i is the number of atoms of each chemical element, and EN_i is the electronegativity of each chemical element in the repeating unit of each polymer.

2.5. Preparation of polymer-haloperidol (HP) solid dispersions

Solid dispersions of polymer-HP were prepared in different repeating unit/drug molar ratios by a solvent evaporation. DMA (1 mL) was used to dissolve 25 mg of HP with varying amounts of each polymer depending on the repeating unit/drug molar ratios. After complete dissolution, the solution was transferred to a petri dish and the solvent was removed by evaporation at 50 °C on a heating base. The resultant solid was kept under vacuum for 72-96 h to remove residual DMA. The absence of residual DMA in solid dispersions was confirmed using ^{1}H NMR spectroscopy.

2.6. Characterization of polymers and solid dispersions

Proton Nuclear Magnetic Resonance (H-NMR)

^{1}H NMR spectra of polymers were recorded with a Bruker spectrometer operating at 250 MHz using methanol-d_4 as the solvent. All chemical shifts are given in ppm.

Powder X-Ray Diffractometry (PXRD)

A small amount of each dry sample (~ 20 mg) was placed on a silica slide and analyzed in a Bruker D8 ADVANCE PXRD equipped with a LynxEye

detector and monochromatic Cu $K\alpha_1$ radiation (λ = 1.5406 Å). Samples were rotated at 30 rpm and data collected over an angular range of 5 to 64° 2θ for 1 h, with a step of 0.05° (2θ) and count time of 1.2 s. The results were analyzed using EVA software.

Differential Scanning Calorimetry (DSC)

Thermal analysis of pure drug, polymers and solid dispersions was performed using DSC (TA Instruments). Samples (3-5 mg) were loaded into pierced T_{zero} aluminum pans. The thermal behavior of each sample was investigated in a nitrogen atmosphere with a heating/cooling rate of 10 °C/min. The values of the glass transition temperature (T_g) of polymers were determined from the second heating cycle. The degree of sample crystallinity was determined by the specific enthalpy (ΔH) of the drug melting peak by TA universal analysis software and calculated as the ratio of the ΔH of drug in the solid dispersions to the ΔH of pure HP. Since the drug content in the dispersion is only a fraction of the sample weight, then the degree of crystallinity was normalized according to the following equation:

$$\text{Crystallinity (\%)} = \left(\Delta H_s * \frac{W_s}{W_h}\right) / \Delta H_h * 100 \qquad (2)$$

where, ΔH_s is the ΔH of the drug in the solid dispersion, having the melting peak around 150 °C (melting point of HP), ΔH_h is the ΔH of pure HP, W_s is the weight of solid dispersions, W_h is the weight of HP in solid

dispersions.

Fourier Transform Infrared (FTIR) spectroscopy

FTIR spectra were recorded on a Nicolet iS5 spectrometer between 4000-400 cm^{-1} at a resolution of 4 cm^{-1} and as an average of 64 scans. The OMINIC software was used for spectral analysis.

2.7. Calculation of solubility parameters

Solubility parameters were calculated using two different methods. The Fedor method (Chokshi et al., 2005; Fedors., 1974; Krevelen, 1990) calculates the solubility parameter δ using the following equation:

$$\delta = \sqrt{\frac{\sum \Delta e_i}{V}} \qquad (3),$$

where Δe_i is the energy of vaporization and V is the molar volume.

The Van Krevelen method (Krevelen, 1990) provides:

$$\delta = \sqrt{\delta_d{}^2 + \delta_p{}^2 + \delta_h{}^2} \qquad (4),$$

where

$$\delta_d = \frac{\sum F_{di}}{V} \qquad \delta_p = \frac{\sqrt{\sum F_{pi}{}^2}}{V} \qquad \delta_h = \sqrt{\frac{\sum E_{hi}}{V}}$$

where δ_d is the contribution from dispersion forces, δ_p is the contribution

from polar forces, δ_h is the contribution of hydrogen bonding, F_{di} is the molar attraction constant due to dispersion component, F_{pi} is the molar attraction constant due to polar component, E_{hi} is the hydrogen bonding energy, and V is the molar volume.

For various groups, the values of Δe_i, F_{di}, F_{pi}, E_{hi}, and V (molar volume) were taken from the literature (Fedors., 1974; Krevelen, 1990).

2.8. In vitro dissolution studies

Dissolution of haloperidol from solid dispersions ([Polymer]/[Drug] = 5:1 mol/mol) used USP Apparatus II (paddle method) at 37±0.5°C with paddles at 50 rpm and simulated gastric fluid (SGF) (0.1 N HCl, pH=1.2). A pharmaceutical grade empty vegan clear capsule size "0" filled with solid dispersion (equivalent to 25 mg drug) was put into the 900 mL SGF with a sinker. Samples (5 mL) were withdrawn at 2, 5, 10, 20, 40, 60, 80, 100 and 120 min, and filtered using a 0.45-μm syringe filter, an equal volume of the SGF was added to the dissolution medium to maintain the volume. The drug was assayed using a UV-visible spectrophotometric method. All dissolution studies were performed in triplicate.

2.9. Statistical analysis

All solid dispersions for each polymer at all drug loadings were prepared

three times independently. All analysis, PXRD, DSC, FTIR as well as dissolution studies, were in triplicate. Data are expressed as mean ± standard deviation.

2. Results and discussion

3.1 Polymer synthesis and characterization

The synthesis of some members of the poly(2-oxazoline) family such as PMOZ with high molecular weights (above 10 kDa) by living cationic ring-opening polymerization is challenging due to the high probability of chain transfer reactions (Litt et al., 1975; Sedlacek et al., 2019b; Wiesbrock. et al., 2005). Recently, Sedlacek et al (Sedlacek et al., 2019b) demonstrated an alternative approach to synthesize well-defined high molecular weight PMOZ through hydrolysis of PEOZ into PEI and subsequent acylation with acetic anhydride.

In this work, a similar strategy was used to synthesize PMOZ, PnPOZ and PiPOZ from commercially-available 50 kDa PEOZ as shown in **Figure 1.**

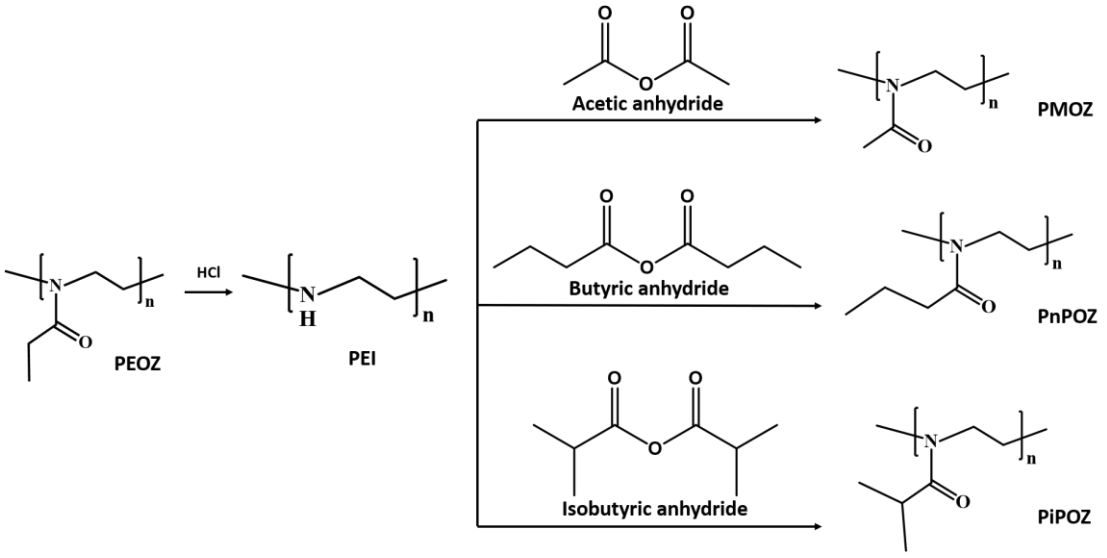

Figure 1. Synthesis of high molar weight PMOZ, PnPOZ and PiPOZ by hydrolysis of PEOZ and subsequent acylation of linear PEI.

The commercial PEOZ was subjected to an acidic hydrolysis of its side chains to yield linear PEI. The full conversion was confirmed by ^{1}H-NMR spectroscopy, where both signals of PEOZ side chains (δ 2.44 ppm and δ 1.13 ppm) were lost and the main backbone signal shifted to δ 2.75 ppm (**Figure S1**). Further confirmation was by FTIR: the loss of the characteristic PEOZ amide carbonyl vibration at 1626 cm^{-1} and the presence of new strong peaks at 1474 cm^{-1} and 3263 cm^{-1} (Fig. S3) assigned to the N-H vibration of PEI again confirmed complete hydrolysis of the amide groups of PEOZ.

The prepared linear PEI was then re-acylated with excess acetic anhydride, butyric anhydride or isobutyric anhydride in DMA using TEA as a base. The resultant PMOZ, PnPOZ and PiPOZ were characterized by ^{1}H-NMR

and FTIR spectroscopies. The ^{1}H-NMR spectra of these polymers show signals corresponding to the poly(2-oxazolines) backbone at 3.5 ppm (peak a, **Figure S1**). The signals labelled as b, c and d are attributed to poly(2-oxazoline) side chains (Boerman et al., 2016; Funtan et al., 2016; Li et al., 2015; Mees et al., 2016; Sedlacek et al., 2019b). Complete conversion from PEI to PMOZ, PnPOZ and PiPOZ was shown not only through the loss of PEI's ^{1}H-NMR signals **(Figure S1)** but also by loss of the PEI's N-H vibration at 3263 cm^{-1} in FTIR spectra, with a strong feature appearing at 1626 cm^{-1} corresponding to the amide carbonyl vibration **(Figure S3).** In detail, the FTIR spectrum for PEOZ shows the following bands: 2977 cm^{-1} (CH_2 stretch), 1626 cm^{-1} (C=O stretch), 1470 cm^{-1} (C–H bending), 1420 cm^{-1} (CH bending), and 1240 cm^{-1} (C–N stretch). The spectrum for PEI shows the bands at 3263 cm^{-1} (N-H stretch), 1474 cm^{-1} (N-H bending), 1132 cm^{-1} (C–N stretch) and 750 cm^{-1} (N-H bending) typical for this polymer. The spectra from the different poly(2-oxazoline) derivatives (PMOZ, PEOZ, PnPOZ and PiPOZ) essentially show the same molecular modes, most noticeably the strong C=O stretching mode around 1630 cm^{-1}.

The parent polymer, the intermediate PEI and resulting poly(2-oxazoline) derivatives were also analyzed by differential scanning calorimetry (DSC) and powder X-ray diffraction (PXRD). **Figure 2** shows DSC thermograms for all poly(2-oxazolines), alongside poly(N-vinyl pyrrolidone) (PVP)

which was used as a positive control in subsequent solid dispersion studies. PVP, PMOZ, PiPOZ, PEOZ and PnPOZ show glass transition temperatures (T_g) at 163.1, 82.7, 69.3, 58.9 and 39.4 °C, respectively, in good agreement with the literature (GATICA. et al., 2013; Glassner et al., 2018; Oleszko et al., 2015; Sessa et al., 2011).The decrease in T_g with increasing number of carbon atoms in the side chain in poly(2-oxazoline) series can be explained by the increased flexibility of the longer side-chains. It is clearly seen that T_g values recorded for poly(2-oxazolines) are substantially lower (82.7, 69.3, 58.9 and 39.4 °C) than the T_g of PVP (163.1 °C). Typically, carriers with higher T_g's are regarded as more desirable for preparing solid dispersions because of their greater rigidity and enhanced ability to inhibit drug crystallization (Huang and Dai, 2014).

The DSC analysis of linear PEI showed it melting at 66.2 ℃, also in good agreement with the literature (Saegusa. et al., 1972); no glass transition could be detected for linear PEI, which is consistent with the observations reported by Lambermont-Thijs et al (2010).

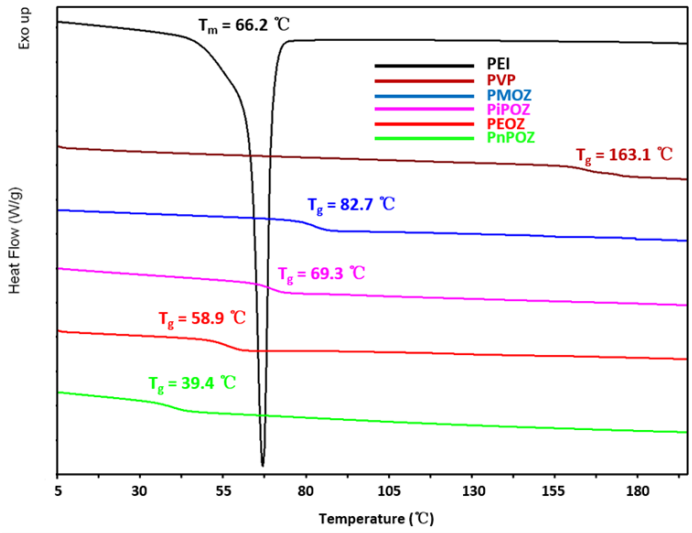

Figure 2. DSC thermograms (second scan) of PVP, PEOZ and synthesized PEI, PMOZ, PnPOZ and PiPOZ showing decreasing glass transition temperatures with increasing numbers of carbon atoms in the side chain.

Due to the absence of side groups and the presence of both hydrogen bond donating and accepting –NH- groups, linear PEI has a strong tendency to crystallize (Lambermont-Thijs. et al., 2010), which was confirmed here by PXRD (**Figure 3**): three main crystalline peaks were observed at 2θ =18.7°, 20.7°and 27.9°.

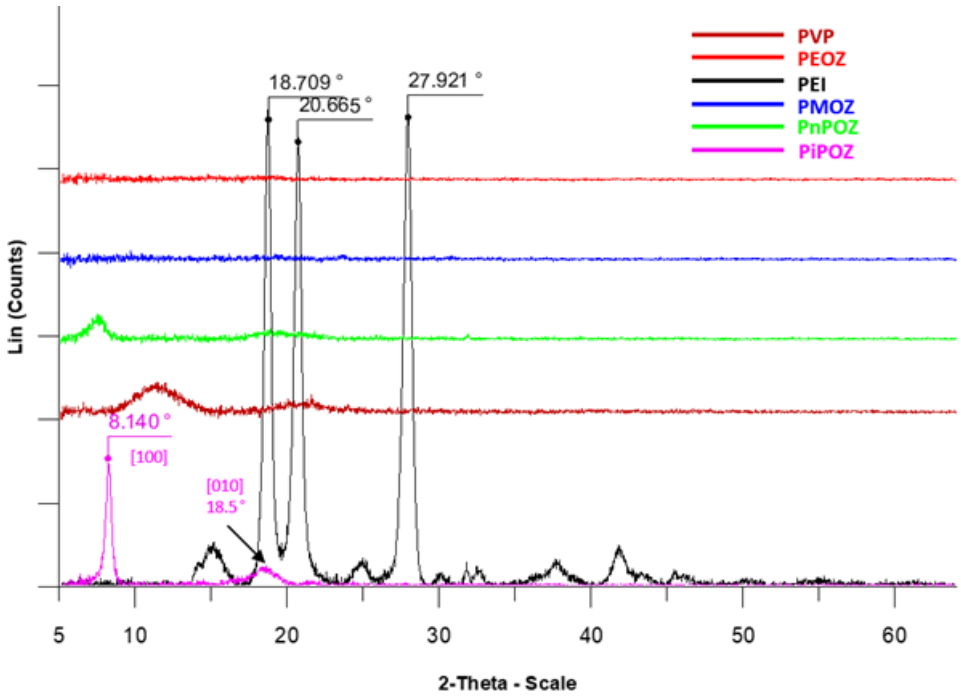

Fig. 3. X-ray diffraction diffractograms of PVP, PEOZ and synthesized PEI, PMOZ, PnPOZ and PiPOZ.

It is interesting that, by x-diffractometry, PiPOZ appears to be semi-crystalline. By DSC, a melting peak occurred at 203.5 °C during the first heating cycle, which was lost during a subsequent second scan, possibly as a result of thermal disruption of crystallinity at higher temperature, as seen in Fig.S2 (Demirel et al., 2007). According to the PiPOZ unit cell model proposed (Demirel et al., 2007; Oleszko et al., 2015), the isopropyl groups alternately align along the [100] direction (the sharp peak at 2θ =8.14°) to either side of the backbone, with the amide dipoles alternately oriented along the [010] direction (the other broad peak at 2θ =18.5°) **(Figure 3).**

The significantly different T_g values for the isomers PiPOZ (69.3℃) and PnPOZ (39.4 ℃) as well as PiPOZ's semi-crystalline nature can be attributed to the different d-spacing (distance between the main chains) together with the more compact isopropyl groups that are less flexible than the n-propyl groups, thereby facilitating their packing into crystallites (Demirel et al., 2016).

PXRD results also confirmed that PVP, PMOZ, PEOZ and PnPOZ are predominantly amorphous.

3.2 Preparation and characterization of solid dispersions

In order to evaluate the effects of different polymers on the crystallinity of haloperidol (HP), solid dispersions (SDs) were prepared by solvent evaporation and were characterized by DSC, PXRD and FTIR, with DSC and PXRD used to calculate the crystallinity of HP in the dispersions. Differences in solvent polarities, boiling points and the evaporation rate all affect the interaction of the drug with polymer. Thus, several solvents and solvent mixtures were initially screened including DMA, ethanol, acetone, chloroform, chloroform-ethanol mixtures and acetone-ethanol mixtures. Only DMA acted as a common solvent to dissolve all polymers and HP.

The X-ray diffractogram of HP **(Figure 4)** shows multiple distinctive peaks, notably at 6.6°, 11.9°, 13.1°, 15.1°, 16.4°, 20.0°, 22.8°, 24.9°, 26.3° and

31.9°, demonstrating the crystalline structure of pure HP.

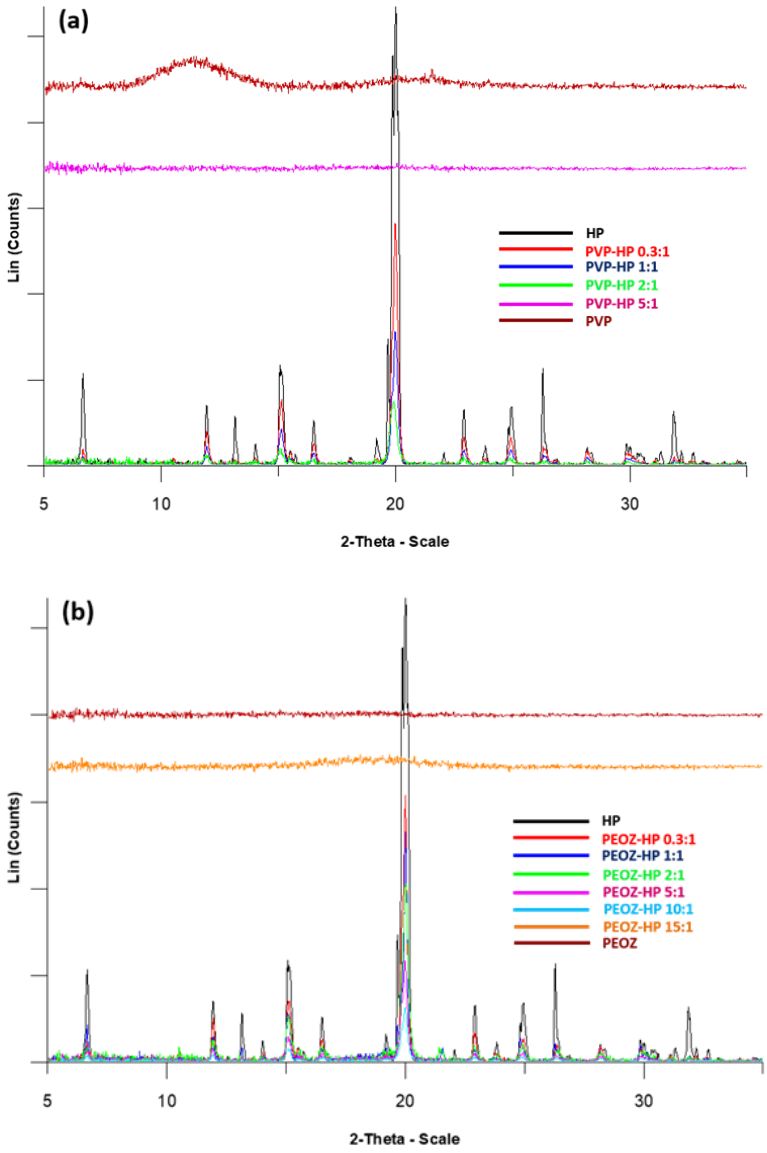

Figure 4. X-ray diffraction diagrams of PVP-HP SDs (a) and PEOZ-HP SDs (b).

A gradual decrease in the drug crystallinity was observed in solid dispersions as the quantity of each polymer increased. For example, solid dispersions with PVP showed the presence of crystalline HP at the

following molar ratios [PVP]/[HP]= 0.3:1, 1:1 and 2:1. A fully amorphous solid dispersion was observed only at [PVP]/[HP]=5:1 **(Figure 4a).** Solid dispersions with PEOZ and PnPOZ showed the presence of crystalline HP at [PEOZ]/[HP] and [PnPOZ]/[HP] molar ratios of 0.3:1, 1:1, 2:1, 5:1 and 10:1 but were amorphous at 15:1 (**Figure 4b and Figure S4b**).

It is interesting to note that when PiPOZ was used to prepare solid dispersions, haloperidol was amorphous only when the [PiPOZ]/[HP] molar ratio reached 20:1 (**Figure S4c**). PXRD analysis of these dispersions revealed that the peak at 2θ =8.14° representing the crystalline domains of PiPOZ strengthened with increasing concentrations of polymer [PiPOZ]/[HP] from 0.3:1 to 15:1. However, when the drug was amorphous at [PiPOZ]/[HP]=20:1, the intensity of the polymer-derived crystalline peak decreased (Figure S4c). This indicates that the crystalline domains of PiPOZ are also affected by the interaction with HP. Interestingly, a new peak that appeared at 2θ=7.8° in PnPOZ-HP dispersions (Figure S4b) suggesting that the interactions with the drug had also increased the crystallinity of the polymer. X-ray analysis of the dispersions formed using PMOZ shown that HP remains crystalline even at the lowest drug loading of [PMOZ]/[HP]=25:1(Fig. S4a).

FTIR spectroscopy was used to investigate molecular interactions between the drug and the polymers in these solid dispersions. Hydrogen bonding

was expected between the hydroxyl group of HP with carbonyl groups of PVP (Chadha. et al., 2006) or with nitrogen atoms of POZ (Moustafine et al., 2019). Such interactions can be confirmed by broadening and shifting in the absorption bands of the interacting groups (He et al., 2004). **Figure 5** presents example spectra of haloperidol, PVP and PVP-HP solid dispersions (2:1 and 5:1) between 1550-1750 cm^{-1} which demonstrates these interactions and **Figure S5** shows all other spectra in a broader spectral region.

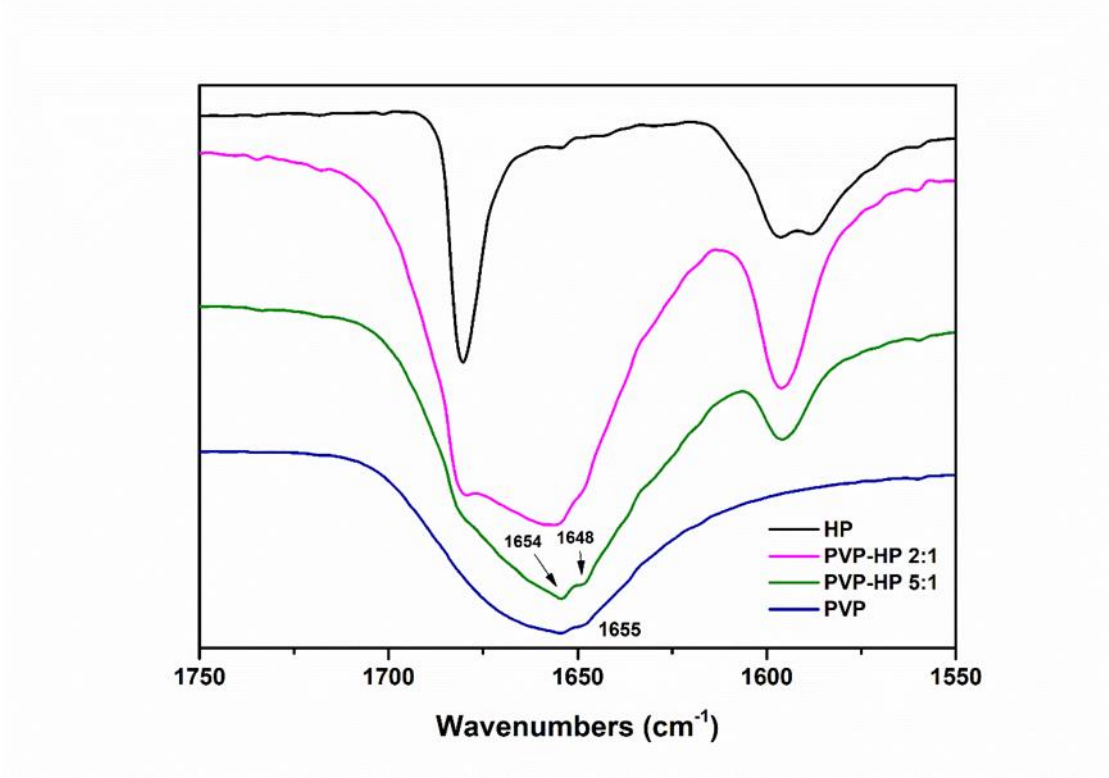

Figure 5. FTIR spectra of HP, PVP and PVP-HP solid dispersions in the range of 1750 - 1550 cm^{-1}.

The spectrum of HP showed characteristic peaks at 3100 cm^{-1} assigned to

the hydroxyl group, 1680 cm^{-1} assigned to carbonyl group and 1595 cm^{-1} due to the benzene ring. Characteristic carbonyl peaks are observed in POZ and PVP spectra at 1626 cm^{-1} and 1655 cm^{-1}, respectively. The HP hydroxyl group peak at 3100 cm^{-1} was lost concomitantly with a broad peak at 3408 cm^{-1} forming as the molar ratio [PVP]/[HP] increased to 2:1. This new broad peak shifted to 3440 cm^{-1} as the molar ratio increased to 5:1, suggesting a change in the environment of the hydroxyl groups, potentially due to hydrogen bonding between the drug and PVP. This is in good agreement with the study reported in (Saluja et al., 2016). Similar loss of the 3100 cm^{-1} peak and a shift to higher wavenumber also observed in POZ-HP spectra, but proof of hydrogen bonding between the drug and poly(2-oxazolines) is confounded since the peak around 3400 cm^{-1} can also be attributed to water, considering the hydrophilic nature of these polymers. Moreover, there was neither peak shifting nor broadening observed for the amide groups in the spectra of solid dispersions, suggesting that very weak or no hydrogen bonding exist between the drug and the poly(2-oxazolines). This is exemplified by comparing FTIR spectra from PEOZ-HP physical mixtures and solid dispersions (15:1) (**Figure S6**). The spectrum of the physical mixture clearly shows characteristic peaks of both PEOZ and the drug, notably the 1680 cm^{-1} feature assigned to the drug carbonyl group and the broad 1626 cm^{-1} peak assigned to the same mode in PEOZ. Though the peaks overlap, these features are also apparent at the same wavenumber

values in the solid dispersion, and the amide feature at 1595 cm^{-1} was also invariant again providing no evidence for significant hydrogen bonding between the drug and carrier.

DSC experiments were also conducted to further investigate the thermal behavior of the solid dispersions. The DSC thermogram of pure HP showed a single characteristic melting peak at 150 °C, confirming its crystalline nature **(Figure 6)**, and in agreement with previous reports (Solanki et al., 2018; Yasir et al., 2016). The DSC curves of solid dispersions showed broader and reduced melting peaks corresponding to the crystalline drug as the amounts of polymer in the dispersions increased **(Figure 6 and Figure S7)**. The HP melting peak was absent in solid dispersions with [PVP]/[HP]=5:1 **(Figure 6a)**, [PEOZ]/[HP]=15:1 **(Figure 6b)**, [PnPOZ]/[HP]=15:1 **(Figures S7c and 7d)** and [PiPOZ]/[HP]=20:1 (**Figure S7b**), indicating that the drug was amorphous. However, HP was still crystalline in the dispersions with PMOZ even at [PMOZ]/[HP]=25:1, in agreement with the earlier X-ray data **(Figure S7a)**.

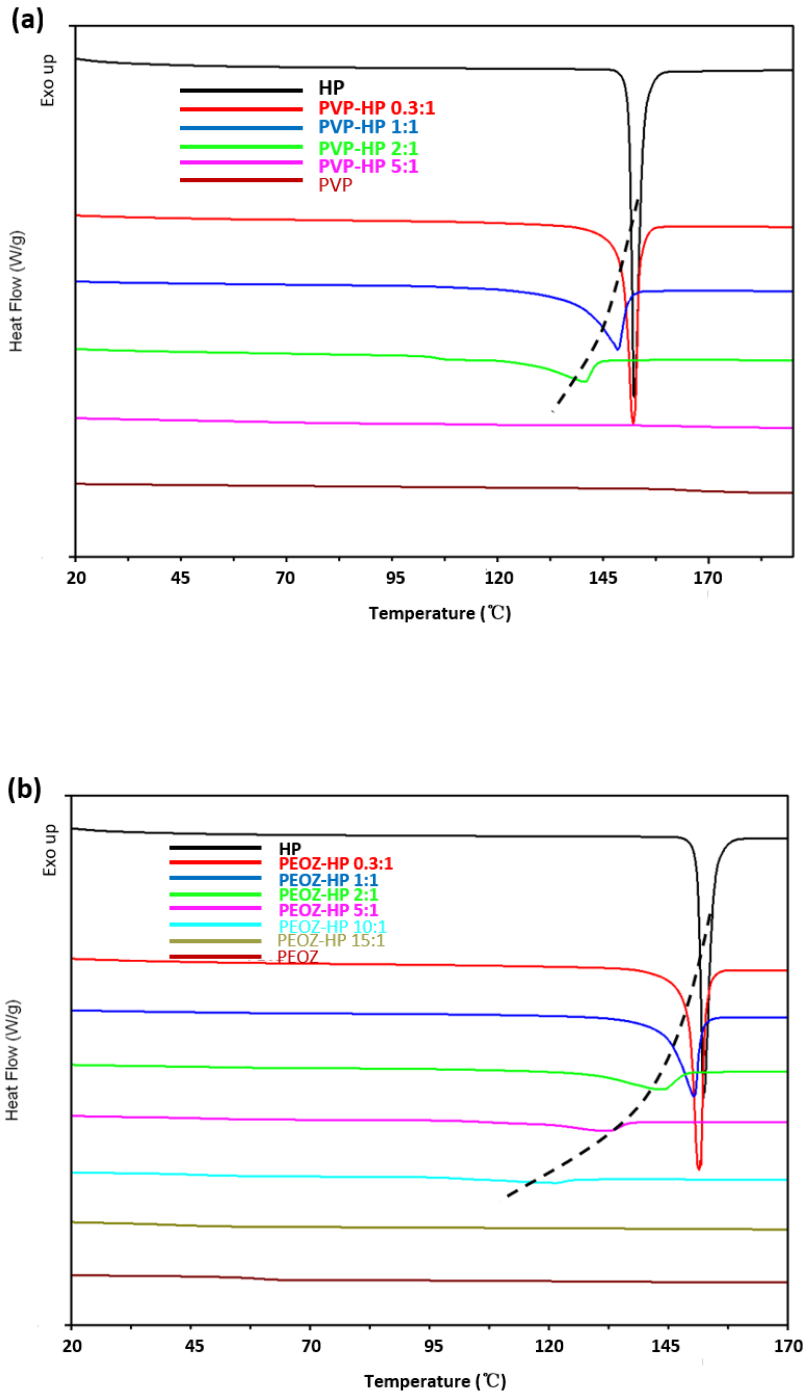

Figure 6. DSC thermograms of PVP-HP (a) and PEOZ-HP (b) solid dispersions. Dashed curve shows the trend in the endothermic events.

As can be seen from **Figure S7b**, **Figure S8 and Table S2**, as the amount of PiPOZ increased, a second endothermic peak appeared at

[PiPOZ]/[HP]= 5:1, 10:1, 15:1 and 20:1, which could be attributed to the crystalline nature of PiPOZ. PiPOZ apparently became increasingly crystalline up to [PiPOZ]/[HP]=15:1, but the polymer crystallinity fell at a ratio of 20:1 where HP crystallinity was lost (Figure S8). Confirming the earlier X-ray studies, the thermal data also suggests that the crystallinity of PiPOZ was affected by interaction with HP. The parameters of peak 2 including the T_m, ΔH_s and degree of crystallinity calculated using equation (S1) and equation (S2) are summarized in **Table S2**.

It is worth noting that there were also two melting peaks apparent in the DSC curves of PnPOZ-HP (1:1, 2:1, 5:1 and 10:1). The T_m of the two peaks obtained from the second cycle after quenching using different method are summarized in Table.S1. The T_m of peak 2 was around 112 °C at 1:1, 2:1 and 5:1, whereas the T_m of peak 1 corresponding to HP decreased from 150.9 ℃ at 1:1 to 134.6 ℃ at 5:1 as the crystalline HP was disordered as it distributed and interacted with the polymer. At a polymer:drug ratio of 10:1, only a single melting event was seen as the two peaks combined. When the first heating cycle temperature was raised from 100 to 120 °C, and then cooled, this melting event was lost from the thermogram. It is extremely unlikely that the peak results from a polymorph of HP since none have been reported to date. For example, a search of the Cambridge Structural Database V5.40 (Groom et al., 2016) revealed only a single, monoclinic crystalline form of HP and an extensive search of the literature

found no evidence to support the existence of another known polymorphic form. Indeed, a recent review by Santos (Santos et al., 2014) identified HP as having only a single known crystalline form. As such, it is unlikely that the broad peak at $2\theta=7.8^{\circ}$ is attributable to a previously unreported crystalline form of HP. Rather, given its broad nature, it seems more likely that this diffraction feature is attributable to crystallization of the polymer. The crystalline character of PnPOZ formed in PnPOZ-HP SDs might result from the interaction with the drug such that the arrangement or density of the polymer has been changed, for example, increasing the average distance between the amide dipoles of different polymer chains could decrease the average strength of dipolar interactions. Weaker dipolar interactions would allow faster relaxation of the PnPOZ chain backbones towards equilibrium crystalline structures. Additionally, the three carbon atoms in the propyl side chain has been reported as the critical number between amorphous and crystalline poly(2-oxazolines) (Demirel et al., 2016). The balance between amorphous PnPOZ and crystalline PnPOZ might be broken because of the involvment of HP. The loss of the second melting peak might be explained by thermal damage to the polyamide at higher temperatures which would also explain the loss of melting peak of PiPOZ in the second cycle after quenching. Although the specific crystallinity of PnPOZ in solid dispersions cannot be calculated because pure PnPOZ is amorphous, it can be seen from the enlargement of Figure

S7c that PnPOZ crystallinity increases with increasing PnPOZ-HP molar ratio from 1:1 to 5:1. Nevertheless, it became amorphous again at 15:1 where the drug also became amorphous, probably because the drug content was below a level where it impacted on the gross structure of PnPOZ.

All T_g of PMOZ-HP SD, PiPOZ-HP SD and PEOZ-HP SD and PnPOZ-HP SD at 15:1 were below the T_g of the pure polymer (**Figure 7**). The decreased T_g was likely resulting from plasticization caused by the interaction of the polymer with drug molecules.

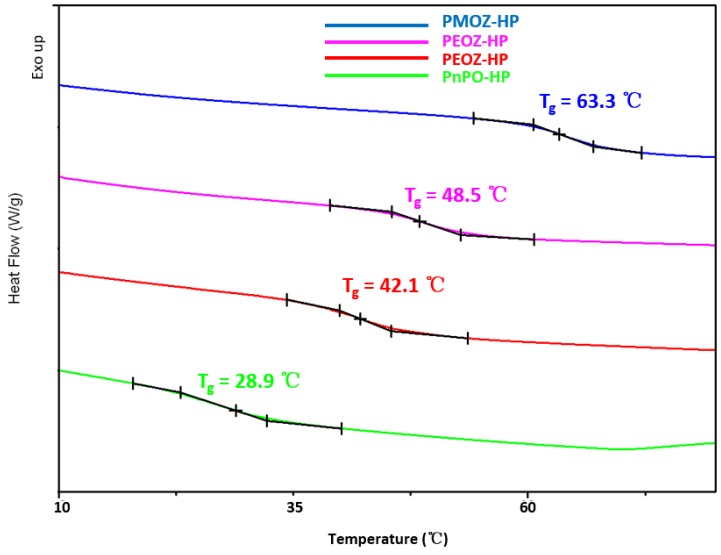

Figure 7. DSC thermograms of solid dispersions formed by PMOZ, PiPOZ, PEOZ and PnPOZ at [polymer]/[drug]=15:1 molar ratio.

PVP is often used as a standard for preparing solid dispersions due to its high hydrophilicity and ability to form stable dispersions (Chadha. et al., 2006; Sharma. and Jain., 2010). However, there are some reports

introducing poly(2-oxazolines) such as PEOZ as dispersion carriers (Boel et al., 2019; Fael et al., 2018). Therefore, PEOZ, PMOZ, PnPOZ and PiPOZ were studied and compared with each other and with PVP. The drug crystallinity in polymer-haloperidol solid dispersions was calculated by the specific enthalpy of the melting peak. As can be seen from **Figure 8**, HP crystallinity was reduced in all dispersions with PVP and was essentially amorphous at a molar ratio of 5:1. By contrast, the HP in solid dispersions with poly(2-oxazolines) had a lower propensity to be disordered and was amorphous at the higher polymer-drug ratio of 15:1.

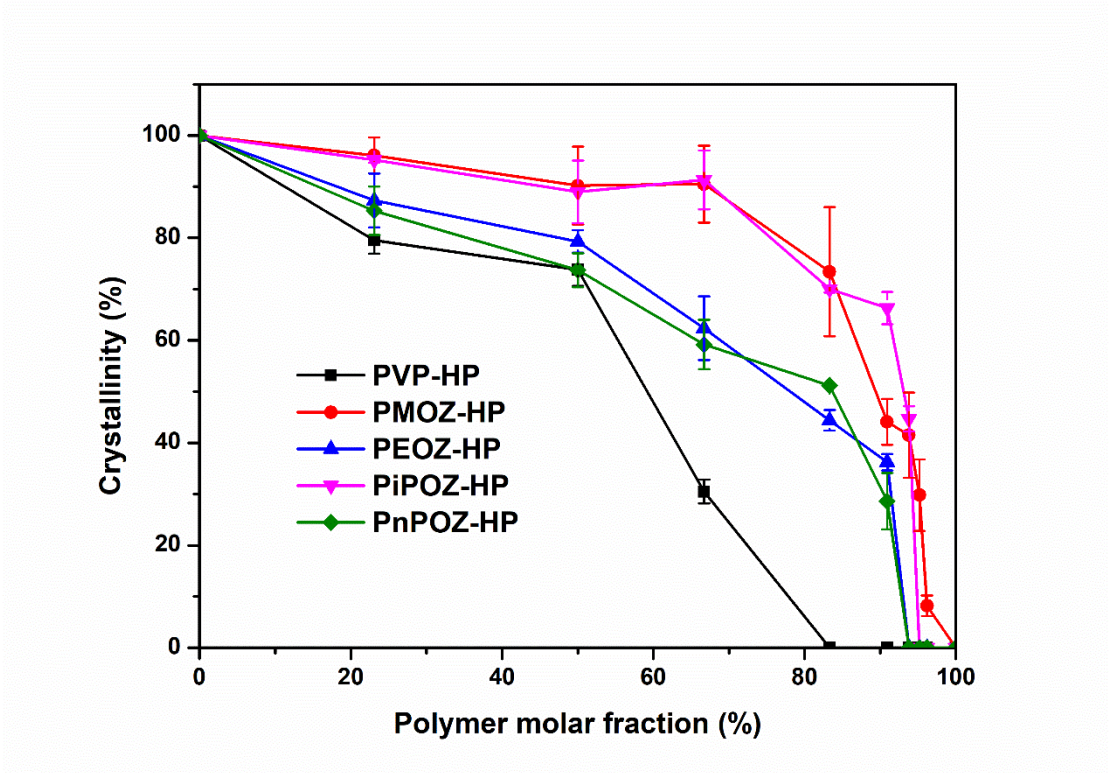

Figure 8. Crystallinity of polymer-HP solid dispersions as a function of polymer molar fraction.

The differing effects are believed to result from the stronger hydrogen-accepting ability of PVP compared to POZ. Oxygen atoms in the tertiary amide group of PVP and nitrogen atoms in the tertiary amide group of POZ can act as hydrogen acceptors to interact with the hydroxyl group of haloperidol via hydrogen bonding. However, the convex and conspicuous cyclic amide group of PVP provides a steric environment that allows its carbonyl group to be more available for hydrogen bonding than the nitrogen atom on the backbone of POZ.

The ability of poly(2-oxazolines) and PVP to reduce the crystallinity of haloperidol has shown an interesting trend that is partially influenced by the hydrophobic-hydrophilic balance (HHB) of each polymer. The most hydrophilic PMOZ (HHB=3.95) has poor ability to reduce crystallinity of haloperidol. The two more hydrophobic members of poly(2-oxazoline) family, PEOZ (HHB=5.02) and PnPOZ (HHB=6.10), have similar and better ability to reduce drug crystallinity. This is logical as non-polar haloperidol molecules will be more likely molecularly dispersed in the hydrophobic domains of PEOZ and PnPOZ. It is interesting to note that PVP has a hydrophobic-hydrophilic balance intermediate between PEOZ and PnPOZ (HHB 5.42), but its ability to reduce drug crystallinity is superior compared to these two polymers. This is possibly related to its better capability to form hydrogen bonds with haloperidol as discussed above.

The ability of PiPOZ, whose HHB is similar to PnPOZ due to their structural isomerism (HHB=6.10), to reduce drug crystallinity is as poor as the most hydrophilic polymer used (PMOZ). The possible reason for this is its semi-crystalline nature, where haloperidol molecules will be less capable of penetrating into densely packed crystalline domains of PiPOZ to form molecular dispersion. **Figure 9** schematically shows the difference in the structure of solid dispersions formed by fully amorphous and semi-crystalline polymers.

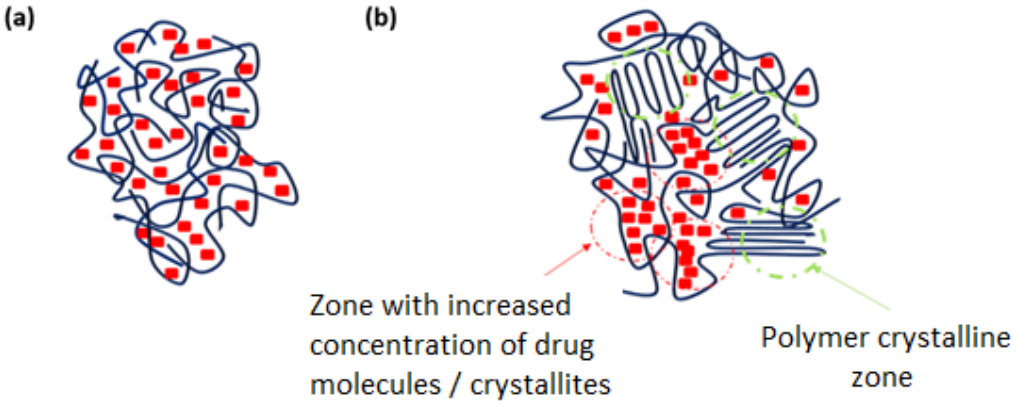

Figure 9. Structures of solid dispersions formed by fully amorphous (a) and semi-crystalline (b) polymers. Red tetragonal symbols represent drug molecules and curved lines represent polymer chains

3.3 Theoretical evaluation of drug-polymer miscibility

The miscibility between haloperidol and the polymers was estimated using the Fedor and Van Krevelen methods. The calculated solubility parameters for haloperidol, PVP, PMOZ, PEOZ, PnPOZ and PiPOZ are in Table 1.

Table 1. Solubility parameters of drug and polymers.

Drug and Polymers	Solubility parameters (δ) ($MPa^{1/2}$)				
	Fedor method	Van Krevelen Method	Average	Δδ	Group classification
Haloperidol	24.3	24.0	24.2		
PVP	26.0	26.3	26.2	2.0	Miscible
PMOZ	26.3	27.0	26.7	2.5	Miscible
PEOZ	24.7	24.5	24.6	0.4	Miscible
PnPOZ	23.7	22.9	23.3	0.9	Miscible
PiPOZ	23.3	22.5	22.9	1. 3	Miscible

Compounds with similar values of δ are more likely to be miscible, because the cohesive energy within each component is balanced by the energy released by interactions between the components. It has been demonstrated

that two compounds with a $\Delta\delta<7.0$ $MPa^{½}$ are likely to be miscible in the molten state whereas compounds with $\Delta\delta>10.0$ $MPa^{½}$ are likely to be immiscible (Greenhalgh. et al., 1999). It can be seen from Table 1 that all the polymers are expected to be miscible with haloperidol with $\Delta\delta$ values ranging from 0.4 to 2.5. Interestingly, solubility parameters for PEOZ and PnPOZ most closely match that of haloperidol, and these polymers showed greatest crystallinity inhibition compared to the other poly(2-oxazolines). However, the discrepancy in $\Delta\delta$ with PVP is 2, yet this polymer showed the greatest crystallinity inhibition efficiency; again, this probably results from hydrogen bond formation between PVP macromolecules and the drug which was absent when using the poly(2-oxazolines) carriers. Further, it should be noted that the solubility parameter approach only considers contact energies between the components and does not allow for the effects of entropy or the free volume of the amorphous state (Jankovic et al., 2019).

3.4. Phase diagrams

According to the Flory-Huggins polymer solution theory (Flory, 1953), a drug-polymer temperature-composition phase diagram can be constructed if the change in drug-polymer interaction parameter χ with temperature is known. The relationship between the melting temperature of the pure drug (T_m^0) and the depressed melting point of the drug in the drug-polymer system (T_m) can be described by the following equation (Huang and Dai,

2014; Lin and Huang, 2010; Moseson and Taylor, 2018):

$$\frac{1}{T_m} - \frac{1}{T_m^0} = -\frac{R}{\Delta H}\left(\ln\phi + \left(1 - \frac{1}{m}\right)(1-\phi) + \chi(1-\phi)^2\right) \quad (5)$$

where R is the gas constant (8.31 J/mol·K), ΔH is the heat of fusion of the pure drug, ϕ is the volume fraction of the drug in the solid dispersion (i.e., drug loading), m is the volume ratio between polymer and drug, and χ is the drug-polymer interaction parameter representing the difference between the drug-polymer contact interaction and the average self-contact interactions of drug–drug and polymer-polymer (Huang and Dai, 2014). A negative χ indicates that the interaction between a polymer and a drug is stronger than the attraction within polymer-polymer and drug-drug pairs. More negative values of χ indicate better affinity between the polymer and the drug and, for example, could be caused by hydrogen bonding between the drug and the polymer. Positive χ values indicate that drug molecules and polymer segments have stronger affinity to interact with those of their own kind rather than interacting with each other (Lin and Huang, 2010).

Equation (5) can be rearranged (Moseson and Taylor, 2018):

$$\left(-\frac{\Delta H}{R}\right)\left(\frac{1}{T_m} - \frac{1}{T_m^0}\right) - \left[\ln\phi + \left(1 - \frac{1}{m}\right)(1-\phi)\right] = \chi(1-\phi)^2$$

$$A = \chi B \quad (6)$$

where A and B values can be derived from melting point depression data. Thus, by measuring melting points of drugs in solid dispersion at different

drug/polymer ratios, a series of A and B values can be generated at different T_m. By plotting A versus B, a χ value can be obtained (**Figure S9**, Supplementary information) and used to predict T_m at any drug/polymer ratio according to equation (5).

The Gordon-Taylor relationship has been used to predict the glass transition in a polymer-drug mixture T_{gmix} (Bruno C. Hancock and Zografi., 1994; Verma and Rudraraju, 2014):

$$T_{gmix} = \frac{W_1 T_{g1} + K W_2 T_{g2}}{W_1 + K W_2} \qquad K = \frac{T_{g1}\rho_1}{T_{g2}\rho_2} \qquad (7)$$

where Tg is glass transition temperature, W_1 and W_2 are the weight fractions of components 1 and 2, and K is calculated from the densities (ρ) and T_g of the respective components.

The data generated through the use of the Flory-Huggins theory and Gordon-Taylor relationship can be used to build the complete phase diagrams (**Figure 10**).

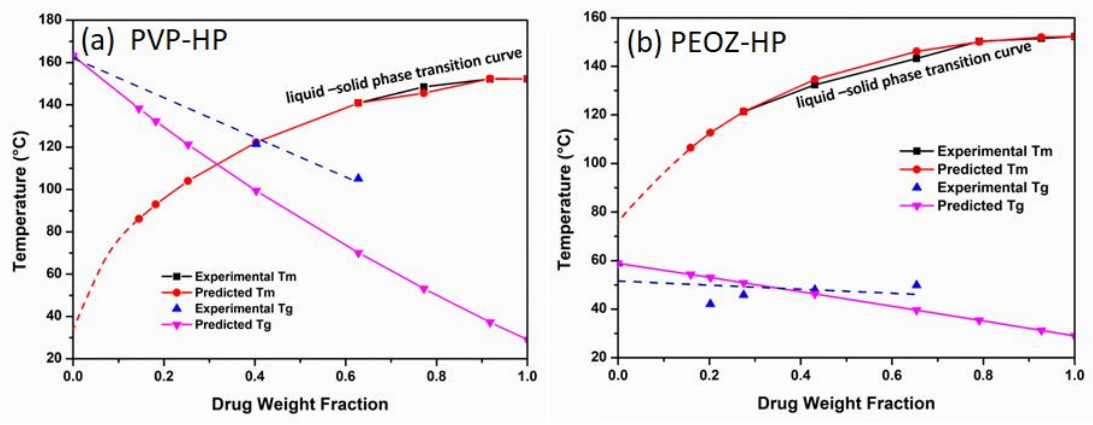

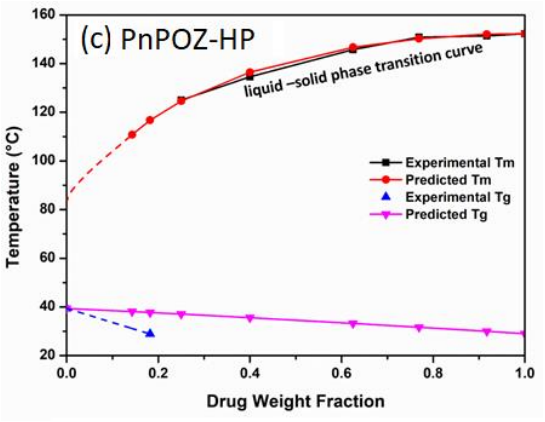

Figure 10. Temperature-composition phase diagrams of polymer-haloperidol solid dispersions showing the experimental and predicted melting temperatures T_m (liquid-solid phase transition curve) as well as experimental and predicted glass transition temperatures. Error bars reflect one standard deviation (n=3) but are within the symbols for the experimental results.

Good agreement of the experimental data and modeled liquid-solid phase transition curve is observed. The negative values of χ=−2.40 for PVP-HP, χ=−1.21 for PEOZ-HP and χ=−0.76 for PnPOZ-HP indicate that these polymer-HP systems are miscible. It is worth noting that the interaction parameter of PVP-HP system showed the most negative value, again related to hydrogen bonding between the drug and polymer chains. However, the A versus B plots for PMOZ-HP and PiPOZ-HP solid dispersions did not give a linear trend (**Figure S9**, Supplementary information) so a single interaction parameter could not be determined and

the phase diagram for these systems could not be build. The interaction parameters at polymer-HP=10:1 and 15:1 mol/mol were positive values, meaning that PMOZ-HP and PiPOZ-HP were not fully miscible. Therefore, based on the values of χ, the solid dispersions can be arranged in the following order from greater drug-polymer interaction to minimal interaction: PVP-HP>PEOZ-HP $\approx$ PnPOZ-HP>PiPOZ-HP $\approx$ PMOZ-HP. It can be clearly seen that this order is consistent with the crystallinity inhibition efficiency of these polymers discussed in section 3.2.

The predicted melting temperature T_m forms the liquid-solid phase transition curve in the phase diagram. The experimental results are in good agreement with the predicted T_m values, but the experimental T_g deviates significantly from the predicted values. This deviation could be related to the presence of specific interactions between the drug molecules and macromolecules. Positive deviations from predicted relationships is typical for strongly interactive systems (Kawakami et al., 2012), whereas negative deviation is observed when the drug-polymer interaction is weaker than drug-drug interaction. Additionally, the presence of water traces in the solid dispersion could contribute to a negative deviation due to plasticization effects (Müllertz et al, 2016).

The liquid-solid phase transition curves were extrapolated to Drug Weight Fraction = 0 (dashed red curves in **Figure 10**). When this curve intersects the T_g curve this allows estimation of the solubility of HP in PVP, PEOZ

and PnPOZ at temperatures where the saturated solutions exist at T_g. It can be seen from Figure 10a that the solubility of HP in PVP is approximately 40% w/w at 122°C and this saturated solution exists at T_g. However, the saturated PEOZ-HP and PnPOZ-HP solutions do not exist at T_g. At room temperature of 25℃, which is characterized by $T<T_m$ and $T<T_g$, these drug/polymer solutions are able to crystallize.

3.5. In vitro dissolution studies

The dissolution profiles of HP and polymer-HP (all 5:1 mol/mol) solid disperisons are presented in **Figure 11**. The dissolution of pure HP within 120 min was below 70%, with 57.3% released in the first 20 minutes. As expected from the crystallinity data (Figure 8), the fastest dissolution was observed from solid dispersions with PVP where haloperidol is essentially amorphous: over 90 % of the drug was released in the first 20 mins. Drug release from solid dispersions with poly(2-oxazolines) was slower compared to PVP, but (other than PnPOZ) faster than HP alone. The release data reflected the fraction of the drug that was amorphous in the dispersions. Thus, solid dispersions with PEOZ which contains ～ 56%:44% amorphous:crystalline haloperidol gave around 80 % of the drug released in 20 mins. Dispersions formed with PMOZ and PiPOZ contain approximately 30% of the drug in an amorphous form and gave statistically similar release profiles with around 70 % drug released in 20 mins. Again,

surprising results were observed for solid dispersions with PnPOZ. Figure 8 shows this system contains approximately 50% of the drug in an amorphous form and so it was expected to exhibit release performance similar to PEOZ; however, its solid dispersions showed even slower dissolution compared to pure crystalline haloperidol, with less than 40% released in 20 mins. This unexpected result could be explained by the Lower Critical Solution Temperature (LCST) in this polymer at ～25 °C (Bouten et al., 2015; Park and Kataoka, 2007) which is much lower than the temperature used in the dissolution studies (37 ℃). Under these conditions PnPOZ remains insoluble in the dissolution medium, which limits drug release from these solid dispersions. Clearly by using polymers that inhibit haloperidol crystallisation, then the generation of supersaturated systems at the dissolution surface or within the bulk fluid is a possibility (Han and Lee, 2017).

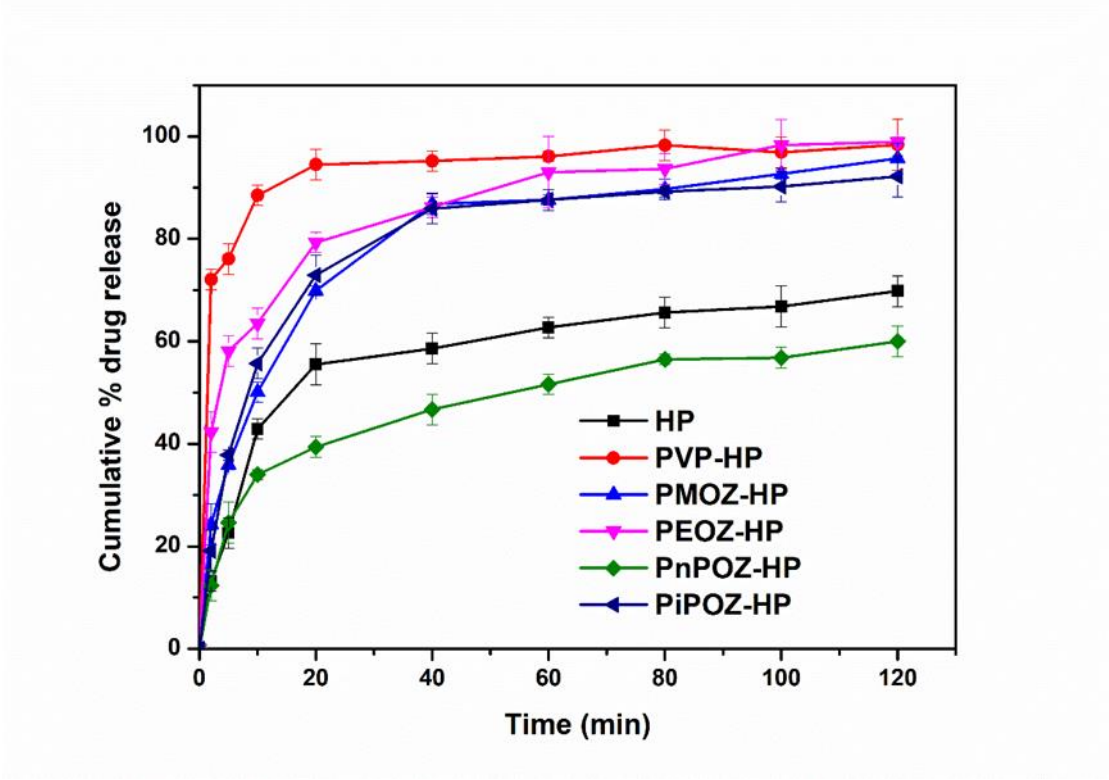

Figure 11. Dissolution profiles of pure haloperidol and from different polymer-haloperidol solid dispersions. Cumulative % drug release with standard error of mean has been plotted against time.

Potentially, more detailed dissolution study of these formulations will be of interest in the future, for example, to evaluate the extent of haloperidol supersaturation on the evolution of kinetic solubility profiles (Han and Lee, 2017).

Conclusion

A series of poly(2-oxazolines) were synthesized in this work by hydrolysis of poly(2-ethyl-2-oxazoline) into poly(ethylene imine) and its subsequent

reaction with acetic, butyric and isobutyric anhydrides. These polymers were fully characterized using ^{1}H NMR and FTIR spectroscopies, differential scanning calorimetry and powder X-ray diffraction.

Solid dispersions of haloperidol were prepared using these poly(2-oxazolines) and poly(N-vinyl pyrrolidone). Polymer structure and properties were found to influence the crystallinity of the drug and its release from solid dispersions. Poly(N-vinyl pyrrolidone) was superior in its ability to reduce crystallinity of haloperidol and gave rapid drug release from solid dispersions. This is related to its ability to form hydrogen bonds with the drug molecules and also with its relatively high hydrophobicity. An increase in the hydrophobicity in a series of poly(2-oxazolines) also favored drug crystallinity reduction. However, poly(2-isopropyl-2-oxazoline) has shown very poor ability to reduce crystallinity of haloperidol, which is related to a semi-crystalline nature of this polymer. The theoretical analysis of these solid dispersions using solubility parameters, Flory-Huggins polymer solution theory and the Gordon-Taylor relationship provided results which are in good agreement with the experimental data.

The dissolution studies indicated good agreement with the levels of drug crystallinity in solid dispersions. However, solid dispersions with poly(n-propyl-2-oxazoline) were found to release drug very slowly due to its lower critical solution temperature and hence insolubility of this polymer in the

dissolution medium. By synthesizing polymers with equivalent degrees of polymerization, the effects of polymer hydrophobic-hydrophilic properties, their semi-crystalline nature, hydrogen bonding strengths, and lower critical solution temperature (influencing polymer solubility) on the structure of solid dispersions and drug release have been demonstrated. Our studies show that, when selecting a carrier for solid dispersions, it is important to consider not only the hydrogen bonding capabilities of the polymer but also its broader properties including their semi-crystallinity, steric properties and lower critical solution temperatures.

Acknowledgments

The authors are grateful to the University of Reading and China Scholarship Council (201707040071) for funding the PhD studentship of X.S. The assistance of staff at the Chemical Analysis Facility (CAF, University of Reading) with ^{1}H-NMR, DSC and PXRD experiments is also acknowledged. The authors are also grateful to Prof Kenneth Shankland for his help in PXRD experiments and valuable advice in interpreting crystallinity data.

Abbreviations used

Poly (ethylene imine) (PEI); Poly(2-alkyl-oxazoline) (POZ); Poly(2-ethyl-2-oxazoline) (PEOZ); Poly(2-methyl-2-oxazoline) (PMOZ); Poly(2-propyl-2-oxazoline) (PnPOZ); Poly(2-isopropyl-2-oxazoline) (PiPOZ); Poly(N-vinyl pyrrolidone) (PVP); Haloperidol (HP); Solid dispersion (SD); N, N-dimethylacetamide (DMA); Triethylamine (TEA); Simulated gastric fluid (SGF).

References

Abu-Diak, O.A., Jones, D.S., Andrews, G.P., 2012. Understanding the performance of melt-extruded poly(ethylene oxide)-bicalutamide solid dispersions: characterisation of microstructural properties using thermal, spectroscopic and drug release methods. Journal of pharmaceutical sciences 101, 200-213.

Ali, W., Williams, A.C., Rawlinson, C.F., 2010. Stochiometrically governed molecular interactions in drug: Poloxamer solid dispersions. International journal of pharmaceutics 391, 162-168.

Baird, J.A., Taylor, L.S., 2011. Evaluation and modeling of the eutectic composition of various drug-polyethylene glycol solid dispersions. Pharmaceutical development and technology 16, 201-211.

Blagden, N., de Matas, M., Gavan, P.T., York, P., 2007. Crystal engineering of active pharmaceutical ingredients to improve solubility and dissolution rates. Advanced drug delivery reviews 59, 617-630.

Boel, E., Smeets, A., Vergaelen, M., De la Rosa, V.R., Hoogenboom, R., Mooter, G.V.D., 2019. Comparative study of the potential of poly(2-ethyl-2-oxazoline) as carrier in the formulation of amorphous solid dispersions of poorly soluble drugs. European journal of pharmaceutics and biopharmaceutics 144, 79-90.

Boerman, M.A., Van der Laan, H.L., Bender, J.C.M.E., Hoogenboom, R., Jansen, J.A., Leeuwenburgh, S.C., Van Hest, J.C.M., 2016. Synthesis of pH- and thermoresponsive poly(2-n-propyl-2-oxazoline) based copolymers. Journal of Polymer Science Part A: Polymer Chemistry 54, 1573-1582.

Brough, C., Williams, R.O., 3rd, 2013. Amorphous solid dispersions and nano-crystal technologies for poorly water-soluble drug delivery. International journal of pharmaceutics 453, 157-166.

Bruno C. Hancock, Zografi., G., 1994. The relationship between the glass transition temperature and the water content of amorphous pharmaceutical solids. Pharmaceutical research 11, 471-477.

Carrier, R.L., Miller, L.A., Ahmed, I., 2007. The utility of cyclodextrins for enhancing oral bioavailability. Journal of controlled release : official journal of the Controlled Release Society 123, 78-99.

Chadha., R., Kapoor., V.K., Kumar., A., 2006. Analytical techniques used to characterize drug-polyvinylpyrrolidone systems in solid and liquid states-An overview. Journal of Scientific & Industrial Research 65, 459-469.

Chaparro, C., Moreno, D., Ramírez, V., Fajardo, A., González, D., Sanín, A., Grueso, R., 2013. Haloperidol as prophylactic treatment for postoperative nausea and vomiting: Systematic literature review. Rev Colomb Anestesiol 41, 34-43.

Chavan, R.B., Rathi, S., Jyothi, V.G.S.S., Shastri, N.R., 2019. Cellulose based polymers in development of amorphous solid dispersions. Asian Journal of Pharmaceutical Sciences 14, 248-264.

Chokshi, R.J., Sandhu, H.K., Iyer, R.M., Shah, N.H., Malick, A.W., Zia, H., 2005. Characterization of physico-mechanical properties of indomethacin and polymers to assess their suitability for hot-melt extrusion processs as a means to manufacture solid dispersion/solution. Journal of pharmaceutical sciences 94, 2463-2474.

Conceicao, J., Adeoye, O., Cabral-Marques, H.M., Lobo, J.M.S., 2018. Cyclodextrins as excipients in tablet formulations. Drug discovery today 23, 1274-1284.

de la Rosa, V.R., 2014. Poly(2-oxazoline)s as materials for biomedical applications. Journal of materials science. Materials in medicine 25, 1211-1225.

Demirel, A.L., Meyer, M., Schlaad, H., 2007. Formation of Polyamide Nanofibers by Directional Crystallization in Aqueous Solution. Angewandte Chemie International Edition 46, 8622-8624.

Demirel, A.L., Tatar Güner, P., Verbraeken, B., Schlaad, H., Schubert, U.S., Hoogenboom, R., 2016. Revisiting the crystallization of poly(2-alkyl-2-oxazoline)s. Journal of Polymer Science Part B: Polymer Physics 54, 721-729.

Demoen., 1961. Properties and analysis of haloperidol and its dosage forms. Journal of Pharmaceutical Scielzces 50, 350-353.

Fael, H., Rafols, C., Demirel, A.L., 2018. Poly(2-Ethyl-2-Oxazoline) as an Alternative to Poly(Vinylpyrrolidone) in Solid Dispersions for Solubility and Dissolution Rate Enhancement of Drugs. Journal of pharmaceutical sciences 107, 2428-2438.

Fedors., R.F., 1974. A Method for Estimating Both the Solubility Parameters and Molar Volumes of liquids.pdf. Polymer Eegineering and Science 14, 147-154.

Flory, P.J., 1953. Principles of polymer chemistry. Cornell University Press.

Funtan, S., Evgrafova, Z., Adler, J., Huster, D., Binder, W.H., 2016. Amyloid Beta Aggregation in the Presence of Temperature-Sensitive Polymers. Polymers 8.

Gatica., N., Soto., L., Moraga., C., Vergara., L., 2013. Blends of Poly(N-vinyl-2-pyrrolidone) and Dihydric Phenols: Thermal and Infrared Spectroscopic Studies. Part IV. Journal of the Chilean Chemical Society 58, 2048-2052.

Glassner, M., Vergaelen, M., Hoogenboom, R., 2018. Poly(2-oxazoline)s: A comprehensive overview of

polymer structures and their physical properties. Polymer International 67, 32-45.

Greenhalgh., D.J., Adrian C. Williams, Peter Timmins, York., P., 1999. Solubility Parameters as Predictors of Miscibility in Solid Dispersions. Journal of pharmaceutical sciences 88, 1182-1190.

Groom, C.R., Bruno, I.J., Lightfoot, M.P., Ward, S.C., 2016. The Cambridge Structural Database. Acta crystallographica Section B, Structural science, crystal engineering and materials 72, 171-179.

Han, Y.R., Lee, P.I., 2017. Effect of Extent of Supersaturation on the Evolution of Kinetic Solubility Profiles. Molecular pharmaceutics 14, 206-220.

He, Y., Ho, C., Yang, D., Chen, J., Orton, E., 2017. Measurement and Accurate Interpretation of the Solubility of Pharmaceutical Salts. Journal of pharmaceutical sciences 106, 1190-1196.

He, Y., Zhu, B., Inoue, Y., 2004. Hydrogen bonds in polymer blends. Progress in Polymer Science 29, 1021-1051.

Hoogenboom, R., 2009. Poly(2-oxazoline)s: a polymer class with numerous potential applications. Angewandte Chemie 48, 7978-7994.

Huang, Y., Dai, W.G., 2014. Fundamental aspects of solid dispersion technology for poorly soluble drugs. Acta pharmaceutica Sinica. B 4, 18-25.

Jankovic, S., Tsakiridou, G., Ditzinger, F., Koehl, N.J., Price, D.J., Ilie, A.R., Kalantzi, L., Kimpe, K., Holm, R., Nair, A., Griffin, B., Saal, C., Kuentz, M., 2019. Application of the solubility parameter concept to assist with oral delivery of poorly water-soluble drugs - a PEARRL review. The Journal of pharmacy and pharmacology 71, 441-463.

Kalepu, S., Nekkanti, V., 2015. Insoluble drug delivery strategies: review of recent advances and business prospects. Acta Pharmaceutica Sinica B 5, 442-453.

Kawakami, K., Usui, T., Hattori, M., 2012. Understanding the glass-forming ability of active pharmaceutical ingredients for designing supersaturating dosage forms. Journal of pharmaceutical sciences 101, 3239-3248.

Khutoryanskiy, V.V., Mun, G.A., Nurkeeva, Z.S., Dubolazov, A.V., 2004. pH and salt effects on interpolymer complexation via hydrogen bonding in aqueous solutions. Polymer International 53, 1382-1387.

Kim, J.Y., Kim, S., Papp, M., Park, K., Pinal, R., 2010. Hydrotropic solubilization of poorly water-soluble drugs. Journal of pharmaceutical sciences 99, 3953-3965.

Knopp, M.M., Nguyen, J.H., Becker, C., Francke, N.M., Jorgensen, E.B., Holm, P., Holm, R., Mu, H., Rades, T., Langguth, P., 2016. Influence of polymer molecular weight on in vitro dissolution behavior and in vivo performance of celecoxib:PVP amorphous solid dispersions. European journal of pharmaceutics and biopharmaceutics : official journal of Arbeitsgemeinschaft fur Pharmazeutische Verfahrenstechnik e.V 101, 145-151.

Krause, M., Huhn, M., Schneider-Thoma, J., Rothe, P., Smith, R.C., Leucht, S., 2018. Antipsychotic drugs for elderly patients with schizophrenia: A systematic review and meta-analysis. European neuropsychopharmacology : the journal of the European College of Neuropsychopharmacology 28, 1360-1370.

Krevelen, D.W.V., 1990. Properties of polymers. Elsevier, 189-221.

Lambermont-Thijs., H.M.L., Bonami., L., Prez., F.E.D., Hoogenboom., R., 2010. Linear poly(alkyl ethylene imine) with varying side chain length_ Synthesis and physical properties. Polym. Chem. 1, 747-754.

Lee, H.L., Vasoya, J.M., Cirqueira, M.L., Yeh, K.L., Lee, T., Serajuddin, A.T., 2017. Continuous Preparation of 1:1 Haloperidol-Maleic Acid Salt by a Novel Solvent-Free Method Using a Twin Screw Melt Extruder. Molecular pharmaceutics 14, 1278-1291.

Li, T., Tang, H., Wu, P., 2015. Molecular Evolution of Poly(2-isopropyl-2-oxazoline) Aqueous Solution during the Liquid-Liquid Phase Separation and Phase Transition Process. Langmuir : the ACS journal of surfaces and colloids 31, 6870-6878.

Li, W., Buckton, G., 2015. Using DVS-NIR to assess the water sorption behaviour and stability of a griseofulvin/PVP K30 solid dispersion. International journal of pharmaceutics 495, 999-1004.

Lin, D., Huang, Y., 2010. A thermal analysis method to predict the complete phase diagram of drug-polymer solid dispersions. International journal of pharmaceutics 399, 109-115.

Litt, M., Levy, A., Herz, J., 1975. Polymerization of Cyclic Imino Ethers. X. Kinetics, Chain Transfer, and Repolymerization. Journal of Macromolecular Science: Part A - Chemistry 9, 703-727.

Lorson, T., Lübtow, M.M., Wegener, E., Haider, M.S., Borova, S., Nahm, D., Jordan, R., Sokolski-Papkov, M., Kabanov, A.V., Luxenhofer, R., 2018. Poly(2-oxazoline)s based biomaterials: A comprehensive and critical update. Biomaterials 178, 204-280.

Mees, M., Haladjova, E., Momekova, D., Momekov, G., Shestakova, P.S., Tsvetanov, C.B., Hoogenboom, R., Rangelov, S., 2016. Partially Hydrolyzed Poly(n-propyl-2-oxazoline): Synthesis, Aqueous Solution Properties, and Preparation of Gene Delivery Systems. Biomacromolecules 17, 3580-3590.

Morrison, P.W., Connon, C.J., Khutoryanskiy, V.V., 2013. Cyclodextrin-mediated enhancement of riboflavin solubility and corneal permeability. Molecular pharmaceutics 10, 756-762.

Moseson, D.E., Taylor, L.S., 2018. The application of temperature-composition phase diagrams for hot melt extrusion processing of amorphous solid dispersions to prevent residual crystallinity. International journal of pharmaceutics 553, 454-466.

Moustafine, R.I., Viktorova, A.S., Khutoryanskiy, V.V., 2019. Interpolymer complexes of carbopol(R) 971 and poly(2-ethyl-2-oxazoline): Physicochemical studies of complexation and formulations for oral drug delivery. International journal of pharmaceutics 558, 53-62.

Müllertz, A., Perrie, Y., Rades, T., 2016. Analytical techniques in the pharmaceutical sciences. Springer, ISSN 2192-6204

Niemczyk, A.I., Williams, A.C., Rawlinson-Malone, C.F., Hayes, W., Greenland, B.W., Chappell, D., Khutoryanskaya, O., Timmins, P., 2012. Novel polyvinylpyrrolidones to improve delivery of poorly water-soluble drugs: from design to synthesis and evaluation. Molecular pharmaceutics 9, 2237-2247.

Oleszko, N., Utrata-Wesołek, A., Wałach, W., Libera, M., Hercog, A., Szeluga, U., Domański, M., Trzebicka, B., Dworak, A., 2015. Crystallization of Poly(2-isopropyl-2-oxazoline) in Organic Solutions. Macromolecules 48, 1852-1859.

Ozeki, T., Yuasa, H., Kanaya, Y., 1997. Application of the solid dispersion method to the controlled release of medicine. IX. Difference in the release of flurbiprofen from solid dispersions with poly(ethylene oxide) and hydroxypropylcellulose and the interaction between medicine and polymers. International journal of pharmaceutics 155, 209-217.

Qu, X., Khutoryanskiy, V.V., Stewart, A., Rahman, S., Papahadjopoulos-Sternberg, B., Christine Dufes, D.M., Clive G. Wilson, R.L., Carter, K.C., Scha¨tzlein, A., Uchegbu, I.F., 2006. Carbohydrate-Based Micelle Clusters Which Enhance Hydrophobic Drug Bioavailability by Up to 1 Order of Magnitude. Biomacromolecules 7, 3452-3459.

Rawlinson, C.F., Williams, A.C., Timmins, P., Grimsey, I., 2007. Polymer-mediated disruption of drug crystallinity. International journal of pharmaceutics 336, 42-48.

Ruiz-Rubio, L., Alonso, M.L., Perez-Alvarez, L., Alonso, R.M., Vilas, J.L., Khutoryanskiy, V.V., 2018. Formulation of Carbopol((R))/Poly(2-ethyl-2-oxazoline)s Mucoadhesive Tablets for Buccal Delivery of Hydrocortisone. Polymers 10.

Saegusa., T., Ikeda., H., Fujii., H., 1972. Crystalline Polyethylenimine. Macromolecules 5, 108-108.

Saluja, H., Mehanna, A., Panicucci, R., Atef, E., 2016. Hydrogen Bonding: Between Strengthening the Crystal Packing and Improving Solubility of Three Haloperidol Derivatives. Molecules 21.

Santos, O.M.M., Reis, M.E.D., Jacon, J.T., Lino, M.E.d.S., Simões, J.S., Doriguetto, A.C., 2014. Polymorphism: an evaluation of the potential risk to the quality of drug products from the Farmácia Popular Rede Própria. Brazilian Journal of Pharmaceutical Sciences 50, 1-24.

Sedlacek, O., Janouskova, O., Verbraeken, B., Hoogenboom, R., 2019a. Straightforward Route to Superhydrophilic Poly(2-oxazoline)s via Acylation of Well-Defined Polyethylenimine. Biomacromolecules 20, 222-230.

Sedlacek, O., Monnery, B.D., Hoogenboom, R., 2019b. Synthesis of defined high molar mass poly(2-methyl-2-oxazoline). Polymer Chemistry 10, 1286-1290.

Sessa, D.J., Woods, K.K., Mohamed, A.A., Palmquist, D.E., 2011. Melt-processed blends of zein with polyvinylpyrrolidone. Industrial Crops and Products 33, 57-62.

Shah, A., Serajuddin, A.T., 2015. Conversion of solid dispersion prepared by acid-base interaction into free-flowing and tabletable powder by using Neusilin(R) US2. International journal of pharmaceutics 484, 172-180.

Sharma., A., Jain., C.P., 2010. Preparation and characterization of solid dispersions of carvedilol with PVP K30. Res Pharm Sci 5, 49-56.

Singh, A., Van den Mooter, G., 2016. Spray drying formulation of amorphous solid dispersions. Advanced drug delivery reviews 100, 27-50.

Singh, S., Parikh, T., Sandhu, H.K., Shah, N.H., Malick, A.W., Singhal, D., Serajuddin, A.T., 2013. Supersolubilization and amorphization of a model basic drug, haloperidol, by interaction with weak acids. Pharmaceutical research 30, 1561-1573.

Solanki, N.G., Tahsin, M., Shah, A.V., Serajuddin, A.T.M., 2018. Formulation of 3D Printed Tablet for Rapid Drug Release by Fused Deposition Modeling: Screening Polymers for Drug Release, Drug-Polymer

Miscibility and Printability. Journal of pharmaceutical sciences 107, 390-401.

Vasconcelos, T., Marques, S., das Neves, J., Sarmento, B., 2016. Amorphous solid dispersions: Rational selection of a manufacturing process. Advanced drug delivery reviews 100, 85-101.

Verma, S., Rudraraju, V.S., 2014. A systematic approach to design and prepare solid dispersions of poorly water-soluble drug. AAPS PharmSciTech 15, 641-657.

Volkova, T., Kumeev, R., Kochkina, N., Terekhova, I., 2019. Impact of Pluronics of different structure on pharmacologically relevant properties of sulfasalazine and methotrexate. Journal of Molecular Liquids 289, 111076.

Wiesbrock., F., Hoogenboom., R., Leenen., M.A.M., Meier., M.A.R., Schubert., U.S., 2005. Investigation of the Living Cationic Ring-Opening Polymerization of 2-Methyl-, 2-Ethyl-, 2-Nonyl-, and 2-Phenyl-2-oxazoline in a Single-Mode Microwave Reactor. Macromolecules 38, 5025-5034.

Williams, A.C., Timmins, P., Lu, M., Forbes, R.T., 2005. Disorder and dissolution enhancement: deposition of ibuprofen on to insoluble polymers. European journal of pharmaceutical sciences : official journal of the European Federation for Pharmaceutical Sciences 26, 288-294.

Yasir, M., Singh Sara, U.V., Som, I., Singh, L., 2016. Development and Validation of a New HPLC Method for In-vitro Studies of Haloperidol in Solid Lipid Nanoparticles. Journal of Analytical & Bioanalytical Techniques 7, 339.

Zayed, Y., Barbarawi, M., Kheiri, B., Banifadel, M., Haykal, T., Chahine, A., Rashdan, L., Aburahma, A., Bachuwa, G., Seedahmed, E., 2019. Haloperidol for the management of delirium in adult intensive care unit patients: A systematic review and meta-analysis of randomized controlled trials. Journal of critical care 50, 280-286.